23rd ABCM International Congress of Mechanical Engineering
December 6-11, 2015, Rio de Janeiro, RJ, Brazil

EXPERIMENTAL EVALUATION OF THERMAL HYDRAULIC PERFORMANCE OF CARBON NANOTUBES DISPERSED IN DISTILLED WATER IN SINGLE-PHASE FLOW

Enio Pedone Bandarra Filho*
Edwin Martin Cárdenas Contreras **
Abdul Orlando Cárdenas Gómez***

Federal University of Uberlandia, Av. Joao Naves de Avila, 2121 – Uberlandia – MG – Brazil – 38408-514

bandarra@mecanica.ufu.br*
emcardenas.1989@gmail.com**
ing_abdulcardenas@hotmail.com***

Abstract. *This paper deals on thermal-hydraulic performance of multi-walled carbon nanotube (MWCNT) nanoparticles dispersed in distilled water in single-phase flow in a horizontal tube. An experimental facility was built to verify the convective heat transfer coefficient in the transition and turbulent flows as well as the pressure drop. The tests were performed while maintaining constant input temperatures in the section varying from 10 to 20°C, whereas the constant heat flux applied on the wall varied between 10 and 18 kW/m2 and the mass flow rate varied between 20 and 100 g/s. The nanofluids were tested at volume concentrations that varied between 0.12% and 0.24%, where the nanoparticles had distinct aspect ratios of 100, 600, and 2400, respectively. The experimental heat transfer coefficient was evaluated as a function of mass velocity, G, and Reynolds number, where significant differences were observed. Regarding the pressure drop, the nanofluids exhibited pressure drops between 5 and 8.7% greater than that of the base fluid. Finally, a parameter was proposed to evaluate the obtained results, which relates the increase in heat transfer as a function of pumping power.*

Keywords: *Nanofluid, Carbon nanotube, Nanoparticle, Heat transfer.*

1. INTRODUCTION

The miniaturization of heat transfer devices is a common practice, which primarily seeks to improve performance and, consequently, reduce the heat exchanger cost. In addition to these efforts, primarily associated with the technological development of new geometries, the scientific and industrial community has sought to improve upon conventional fluids to create fluids that exhibit a lower thermal conductivity. With the advent of nanotechnology and the eventual possibility of synthesizing materials on a nanometric scale, new initiatives have emerged that seek to improve the thermal properties of working fluids, such as that reported by (Masuda H., *et al*., 1993) Ultra-fine solid particles of Al_2O_3, SiO_2, and TiO_2 have been dispersed in a fluid base via the application of an electrostatic repulsion technique, which increased the thermal conductivity in proportion to the concentration. These ultra-fine particles with dimensions between 1 and 100 nm dispersed in conventional fluids, such as water, oil, or ethylene glycol, are referred to as nanofluids, as described by (Choi S.U.S.,1995). According to the author, nanofluids offer stable dispersions for long periods of time and exhibit a greater thermal conductivity than that of the base fluid. According to (Pak B.C and Cho Y.I, 1998) and (Xuan Y. and Li Q., 2003), convective heat transfer using nanofluids varies depending on the particle properties, dimensions, and volumetric fraction. Due to the promising characteristics of the use of nanofluids, many researchers have studied the performance of heat transfer and the flow characteristics of various nanofluids, where nanoparticles have been produced from different materials and in various base fluids. (Pak B.C and Cho Y.I, 1998), tested nanofluids with Al_2O_3 and TiO_2 in water, where the Nusselt number in fully developed and turbulent flow was shown to increase proportionally with the volumetric concentration and Reynolds number. However, for nanofluids with a 3% concentration, the heat transfer coefficient was 12% lower. (Yu W. et al., 2009), performed experiments with silicon carbide (SiC) nanofluids dispersed in water with a volume concentration of 3.7%. The results showed that the nanofluid compared with water at the same Reynolds number showed an enhancement between 50% and 60%. Using the criteria of constant velocity, the heat transfer coefficient of the nanofluid was 7% lower. (Asirvathama *et al*., 2011), tested silver nanofluids in water. The results showed that the heat transfer coefficient of the nanofluid increased notably, by 28.9% for a concentration of 0.3% and 69.3% for a concentration of 0.9%, and was a function of the Reynolds number. (Sajadi and Kamesi, 2011) experimentally analyzed the TiO_2/water nanofluid. For a Reynolds number of 5000, the heat transfer coefficient of the nanofluid increased by 22% relative to that of the base fluid. (Sundar *et al*., 2012) investigated Fe_3O_4 nanofluids where the average diameter was 36 nm. The results showed that the nanofluid with a concentration of 0.6% and a Reynolds number of 22000 exhibited an increase in the heat transfer coefficient of 31% and an increase in the friction factor of 10% compared with those of water. Recently, (Meyer *et al.*,2013) and (Haghighi *et al.*, 2010), presented an analysis of the heat transfer performance of nanofluids, which used the Reynolds number, flow velocity, and pumping power as criteria for comparison, and the results suggest that the last factor is the most relevant criterion.

2. PROCEDURES AND EXPERIMENTAL SET-UP

In this work, the nanofluids were produced using the 2-step method through the dispersion of multi-walled carbon nanotubes in distilled water. This method requires the use of additional external energy, which was provided by ultrasonication followed by a high-pressure homogenization process to break the agglomerates of nanoparticles and contribute to the homogeneity and stability of the suspension according to (Bandarra Filho *et al.*, 2014). All the nanofluid samples were prepared using the same routine; however, the nanofluids, which are denoted as NT01, NT02, and NT03, contained different aspect ratios, i.e. length by diameter, r=l/d. A 0.5% mass concentration was used for the NT02 and NT03 samples, and a 0.25% mass concentration was used for the NT01 nanofluid. Two and half liters of nanofluid were required to fill the experimental facility and a half-liter reserved for characterization. Figure 1 (a) shows the samples, NT01, NT02, and NT03, which were stable after 10 days, and Fig. 1 (b) shows the images of the MWCNTs obtained by transmission electron microscopy.

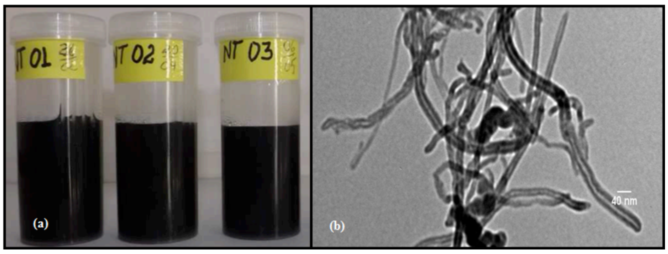

Figure 1. (a) Images of the nanofluids samples: stable after 10 days. (b) Images of the MWCNTs obtained by transmission electron microscopy.

The nanoparticle concentration in the suspension is the parameter whose effect has been frequently evaluated, which is generally referenced as a function of the volume fraction of the nanoparticles, ϕ, as described in Eq. (1).

$$\phi = \frac{V_{np}}{V_{np} + V_{bf}} \tag{1}$$

where V_{np} is the volume of the nanoparticles, and V_{bf} is the volume of the base fluid. The density is given by $\rho=m/V$; the mass of the nanoparticles, m_{np}, which is used to prepare the suspension, is a function of the volumetric concentration of the nanoparticles, ϕ, and the mass of the base fluid, m_{bf}, through Eq. (2).

$$m_{np} = \frac{\phi\, m_{bf}\, \rho_{np}}{(1-\phi)\,\rho_{bf}} \tag{2}$$

Table 2 shows the characteristics of the nanoparticles used in the present study and their respective quantities used in the preparation of each of the nanofluid samples. The multi-walled carbon nanotubes used in this study were acquired from Nanostructured & Amorphous Materials, Inc. (NanoAmor). The values of the specific heat and density of the carbon nanotubes used were c_{pCNTs} = 710 J/kgK and ρ_{CNTs} = 2100 kg/m^3, respectively.

Table 2. Geometric characteristics of the nanofluids used in the present investigation.

Nanofluid	L [μm]	d [nm]	r=L/d	wt [%]	ϕ [%]
NT01	20	30	600	0.25	0.12
NT02	8	80	100	0.50	0.24
NT03	36	15	2400	0.50	0.24

The thermal conductivity of the nanofluid samples was evaluated using the transient hot wire method, also known as a linear probe. A Hukseflux TP-08 probe was used and the samples were measured at a temperature of 22.3°C. The probe, which had been previously calibrated with water, where k = 0.6 W/mK, was completely immersed in the fluid. Three tests were performed for each of the samples analyzed. The measurements were also performed at three other temperatures: 15, 20, and 25°C. Figure 2 shows the experimental results for the thermal conductivity of the nanofluid samples according to the different fluid temperatures used. The conductivity measurement results for NT01, which contained the lowest volumetric concentration of dispersed nanotubes at 0.12% and an aspect ratio (L/d) of 600, exhibited an increase of 6.3% compared with that of the base fluid. Samples NT02 and NT03, which contained the same volumetric concentration of 0.24% but with aspect ratios of 100 (NT02) and 2400 (NT03), exhibited different increases in conductivity, 8.8% and 17%, respectively. Furthermore, the results show the increase in the thermal conductivity of the first two samples (NT01 and NT02) is within the measurement uncertainty range of the device, ± 3% + 0.02 W/mK. According to (Meyer *et al.*, 2013), this is due to the measurement method of the hot wire, which is extremely sensitive to natural convection. It can also be observed that at a temperature of 20°C, the data points essentially follow a straight line, showing that natural convection is reduced for the sample that is being measured.

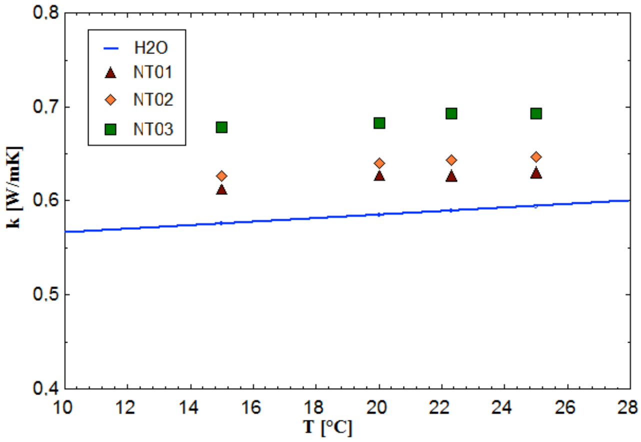

Figure 2. Experimental results of thermal conductivity of distiled water and 3 MWCNT nanofluids according to the temperature.

The viscosity measurements of the samples were performed using a cone-plate rheometer (Brookfield LDDV-IIIU). The equipment measures the shear stress of the sample based on the strain rate imposed and determines the torque necessary to turn the conical element. The dynamic viscosity was measured in a temperature range from 5 to 25°C at an interval of 5°C. Figure 3 illustrates the experimental results for the viscosity of the different samples obtained for different temperatures. Because the three samples, NT02, NT03, and NT04, were produced from carbon nanotubes, it is evident that the sample with the lowest volumetric concentration of nanoparticles (0.12%) will have the lowest effective viscosity, 8.8% in this case. For samples NT02 and NT03, which contained the same volumetric concentration of 0.24%, the effective viscosity exhibited increases of 17.8% for NT02 and 11.6% for NT03.

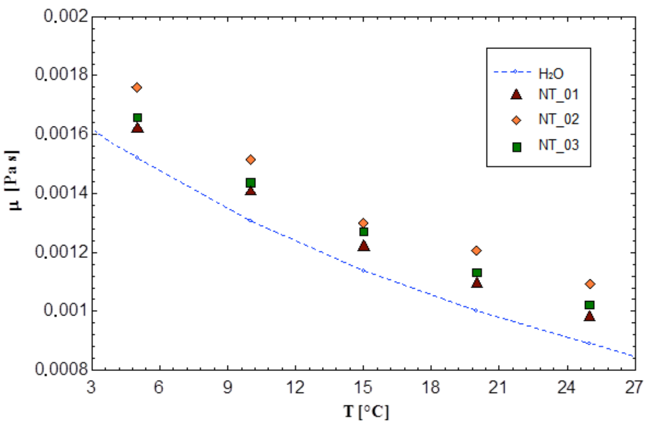

Figure 3. Experimental values of viscosity of distiled water and 3 MWCNT nanofluids with respect to temperature.

In the majority of studies, the density of nanofluids is assumed to be compatible with the theory of mixtures. (Pak B.C and Cho Y.I, 1998), measured the density of samples of a nanofluid composed of titanium dioxide and alumina in water with a nanoparticle concentration of up to 31.6% and found a maximum deviation of 0.6% compared with the results calculated by the theory of the mixture rule. Once the volume concentration of the nanoparticles in the dispersion, ϕ, is determined, the density of the dispersion can be calculated using the following equation:

$$\rho_{nf} = (1-\phi)\rho_{bf} + \phi\,\rho_{np} \tag{3}$$

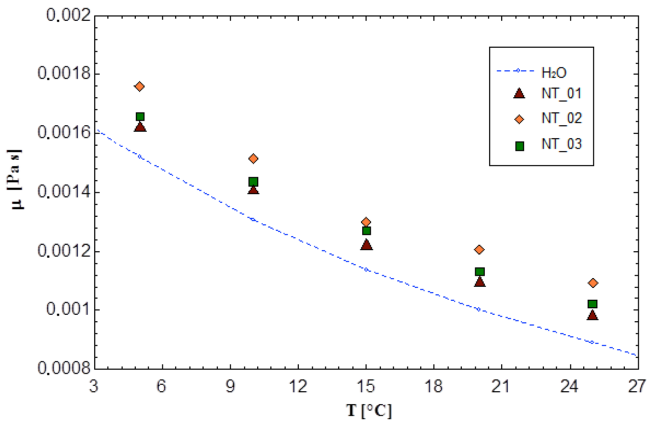

Figure 3. Experimental values of viscosity of distiled water and 3 MWCNT nanofluids with respect to temperature.

(O'Hanley *et al.*, 2012), performed a study on the measurement and validation of a model that calculate the specific heat of nanofluids. It is important to emphasize that the model uses the volume fraction but also considers the thermal capacity of the elements involved in the suspension. This model is given by the following relationship:

$$c_{p,nf} = \frac{(1-\phi)(\rho c_p)_{bf} + \phi(\rho c_p)_{np}}{(1-\phi)\rho_{bf} + \phi\,\rho_{np}} \tag{4}$$

An experimental bench, Fig. 4, was constructed such that it was possible to determine the heat transfer coefficient and the pressure drop in single-phase flow in the transition and turbulent regimes inside a horizontal tube. The test section, through which the nanofluid circulates by the action of a magnetic pump with non-metallic gears, where the speed is controlled by a frequency inverter, consists of a brass circular tube with a smooth interior, a length of 2460 mm, an external diameter of 12.7 mm, and a wall thickness of 3.18 mm. The measurement of the wall temperature along the tube is achieved using 12 type-T thermocouples, which are fixed in grooves made in the tube at different positions. The temperature and pressure conditions at the inlet and outlet are measured by RTD PT100 sensors and piezo-resistive type pressure transducers, respectively. The pressure difference between the inlet and outlet of the test section was also measured using a differential pressure transducer.

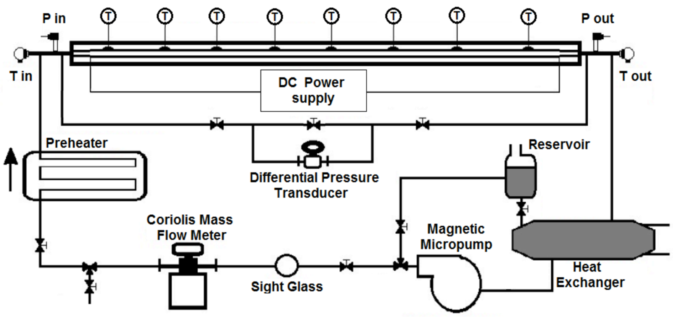

Figure 4. Schematic diagram of the experimental facility.

All the transducers were calibrated using a dead weight tester or column manometer. Each thermocouple and channel of the associated acquisition system was duly calibrated using a thermostatic bath containing a precise thermometer.
A Coriolis-type sensor measures the mass flow rate, which was installed in the primary flow line immediately following the visualization section and before the pre-heater. To obtain the boundary condition of constant heat flux in

the test section, flexible tape-type, 1500-W electrical resistors were used, whose power is provided by a DC electrical source. The thermal insulation of the test section was a layer of rockwool with a thickness of 25 mm.

3. DATA REDUCTION AND RESULTS

The heat transfer coefficient was determined using the following equation:

$$h = \frac{\dot{Q}/A_s}{\Delta T} \quad (5)$$

Where the heat flux, $\dot{Q}$, is the electrical power, A_s is associate to the heating area, and the denominator corresponds to the difference between the temperatures of the tube wall and fluid. The Reynolds and Prandtl numbers were calculated using Eq. (6) and Eq. (7), respectively.

$$\mathrm{Re} = \frac{4\dot{m}}{\pi D \mu} \quad (6)$$

$$\mathrm{Pr} = \frac{\mu C p}{k} \quad (7)$$

where k and μ are the thermal conductivity and viscosity of the working fluid, which were obtained experimentally.
Figure 6 shows a comparison between the heat transfer coefficient obtained experimentally for distilled water and that calculated using the Gnielinski correlation (Gnielinski V.,1976), Eq. (8) and f is the friction factor calculated using the Petukhov correlation, Eq. (9), as follow:

$$Nu = \frac{\frac{f}{8}(\mathrm{Re}-1000)\mathrm{Pr}}{1+12.7\left(\frac{f}{8}\right)^{1/2}\left(\mathrm{Pr}^{2/3}-1\right)} \quad (8)$$

$$f = (0.79\ln(\mathrm{Re})-1.64)^{-2} \quad (9)$$

It is interesting to observe that the average deviation provided by the experimental results in relation to those obtained with the Gnielinski correlation was 5.7%. It is worth emphasizing that the results were surveyed for a mass velocity range between 600 and 3200 [kg/sm^2].

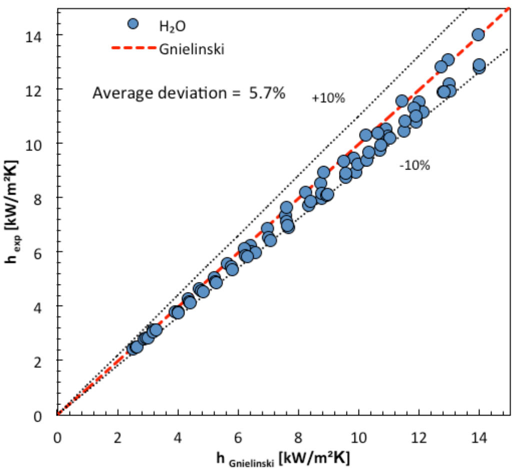

Figure 6. Comparison of the experimental heat transfer coefficient for distilled water in relation to obtained by the Gnielinski correlation.

The friction factor was also used to validate the experimental results, which was calculated using Eq. (10) and later compared with that obtained using the Petukhov correlation (Petukhov B.S and Popov V.N., 1963), i.e., Eq. (13).

$$f = \frac{\Delta P \rho \pi^2 D^5}{8 L \dot{m}^2} \quad (10)$$

where ΔP is the pressure drop determined through the measurements of the differential pressure transmitter. The experimental results shown in Fig. 7 were obtained for distilled water and showed an average deviation of 2.1% in relation to the Petukhov correlation.

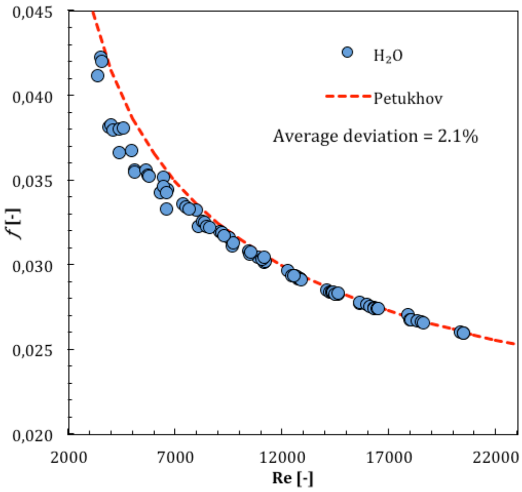

Figure 7: Experimental results for distilled water of the Darcy's friction factor, f_{exp} versus Reynolds number, including the Petukhov correlation.

3.1 Heat Transfer Results

The three types of nanofluids shown in Table 2 were tested for a range of Reynolds numbers between 3000 and 20000, and the following parameters were maintained as nominal imposed conditions: the inlet temperature (with values held constant at 10°C, 15°C, and 20°C), specific heat flux in the test section (varying between 10 and 18 kW/m^2), and mass flow rates (between 20 and 100 g/s with increments of 10 g/s). Figures 8, 9, and 10 show the experimental results obtained for distilled water and the nanofluids in terms of the heat transfer coefficient as a function of the mass velocity and Reynolds number. The primary objective was to verify the primary characteristics provided by these two parameters because, for the same Reynolds number, the heat transfer coefficient of the nanofluid results in a value higher than that obtained for distilled water.
It is interesting to observe in Fig. 8 (a) that sample NT01 (ϕ =0.12% and r=600) with a volume concentration of 0.12% showed a heat transfer coefficient that was, on average, 1.0% lower than the heat transfer coefficient of the base fluid for the same nominal test conditions. However, it can be observed in Fig. 8 (b) that the heat transfer coefficient as a function of the Reynolds number, Re, increased for sample NT01 compared with that of distilled water by approximately 12.5%. This increase is related to the dispersion, which results.
in a higher thermal conductivity due to the addition of the nanoparticles, the developing thermal boundary layer as a consequence of the increase in thermal diffusivity, and the stochastic movements resulting from Brownian motion, which favor the energy exchange process according to Kim et al. [34]. However, this difference cannot be quantified because the experimental parameter adopted for all the tests is mass flow rate.

According to (Pak B.C and Cho Y.I, 1998), the comparison method based on the Reynolds number is not the best method for an effective comparison because the viscosity of the nanofluid is greater than that of the base fluid. According to (Haghighi *et al.*,2014), the comparisons performed for the same Reynolds number suggest that any fluid with an elevated viscosity exhibits greater heat transfer coefficients and can be considered promising as refrigerating fluids. However, the referenced authors propose the pumping power as a method of comparison because both the heat transfer coefficient and the pressure drop of the fluid are considered. Figure 9 (a) illustrates the experimental results for the heat transfer coefficient as a function of mass velocity, G, and Fig. 9 (b) presents the heat transfer coefficient as a function of Reynolds number for distilled water and for sample NT02 (ϕ =0.24% and r=100) for the same test conditions.

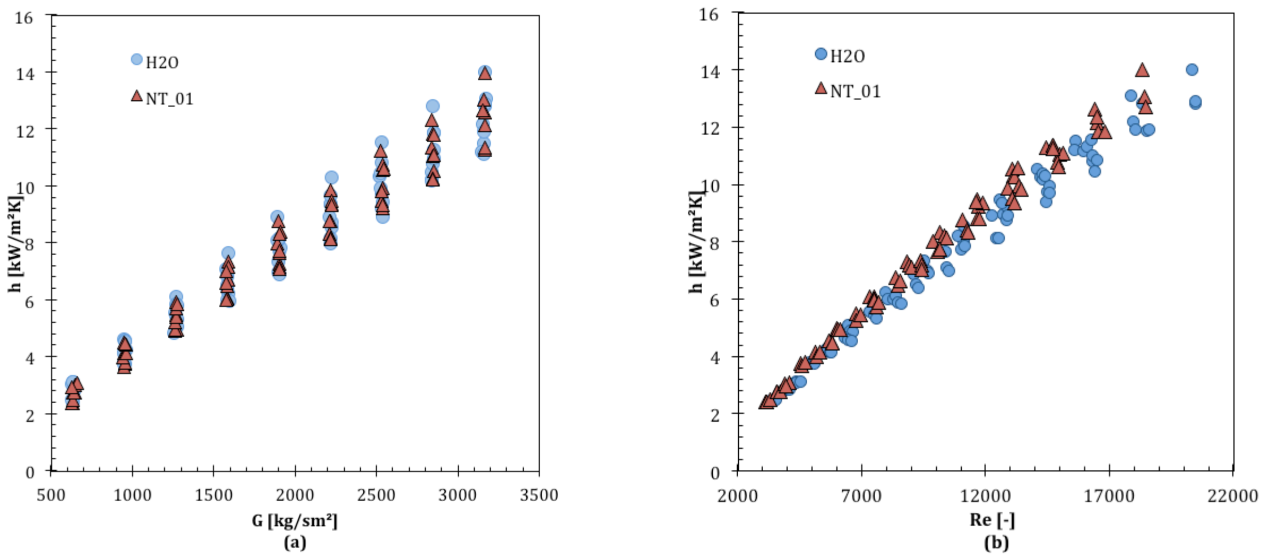

Figure 8: Comparison of the heat transfer coefficient obtained for distilled water and nanofluid NT01 (ϕ=0.12% and r=600) against mass velocity (a) and Reynolds number (b).

It is interesting to observe that the convective heat transfer coefficient is a function of mass velocity, which exhibited a decrease of approximately 2% for NT02 compared with that of the base fluid. As a function of Reynolds number, the heat transfer coefficient for the nanofluid was approximately 27% greater than that obtained for the base fluid.

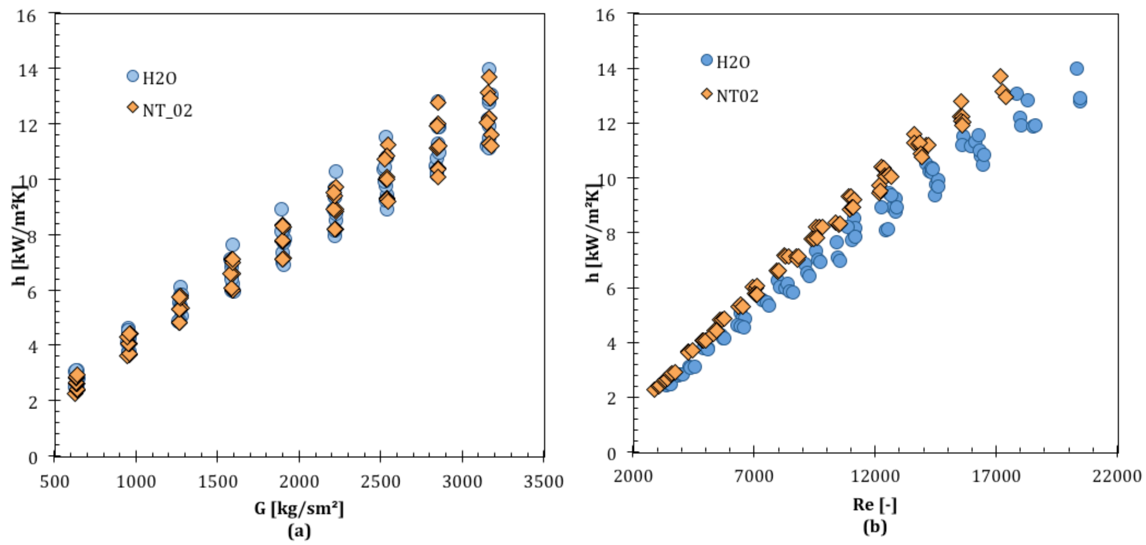

Figure 9: Comparison of the heat transfer coefficient obtained for distilled water and nanofluid NT02 (ϕ=0.24% and r=100) against mass velocity (a) and Reynolds number (b).

According to Fig. 10 (a), sample NT03 (ϕ = 0.24% and r=2400) exhibited an average heat transfer coefficient increase of 6% as a function of mass velocity compared with that obtained with the base fluid. In Fig. 10 (b), where the heat transfer coefficient is presented as a function of Reynolds number, it is possible to verify the clear increase in the heat transfer coefficient of 30%. It is important to highlight that the Reynolds number is calculated from the thermophysical properties of the tested sample (according to the procedure described in section 2), where it was, on average, 10.4% lower than that of water for the tests performed at the same nominal conditions.

As observed in Fig. 10 (b), the increase observed in the heat transfer coefficient by sample NT03 is due to its greater aspect ratio of r=2400. At these conditions, the nanoparticles have a lower average diameter, which, when related to the length, provides a larger specific area that favors Brownian motion that consequently results in stochastic movements of the particles in the fluid, which benefits the energy exchange process. Another advantage of the nanoparticles with a higher specific area is that there is a greater proximity of the liquid molecules with the surface of MWCNTs, which, according to Jiang et al. (2009), can increase the thermal conductivity of the nanofluid, also benefitting energy exchange.

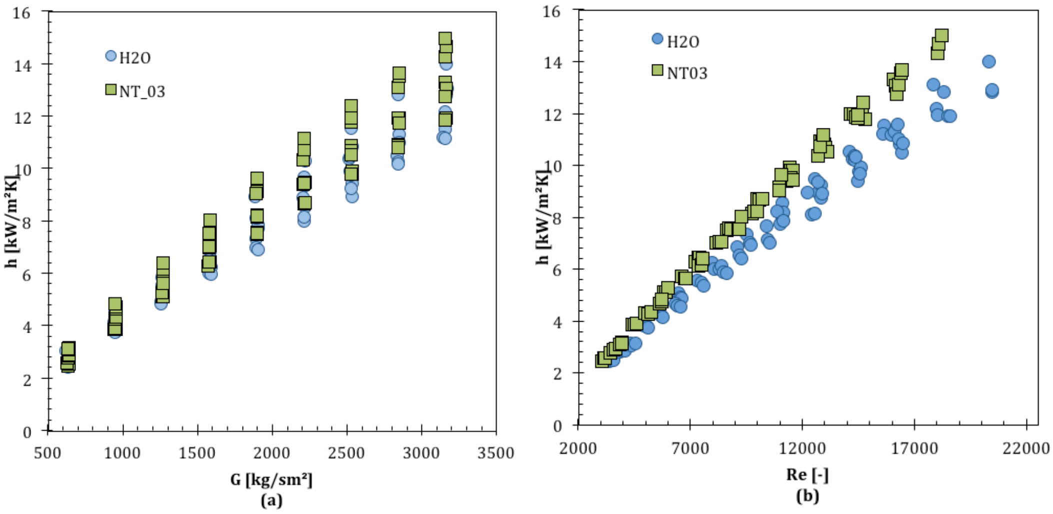

Figure 10: Comparison of the heat transfer coefficient for distilled water and nanofluid NT03 (ϕ = 0.24% and r=2400) against mass velocity (a) and Reynolds number (b).

3.2 Pressure Drop and Friction Factor

The pumping power values were calculated according to the values of the pressure drop for each condition of the mass flow rate tested. The friction factor was calculated using Eq. (10), and the results were compared with that obtained using the Petukhov correlation, Eq. (9). Figure 11 shows the values obtained experimentally for the friction factors as a function of the Reynolds number for the nanofluids, which includes the Petukhov correlation obtained for distilled water. As observed, the friction factor of the nanofluid samples were compared with those obtained using the Petukhov equation, which provides an average deviation for samples NT01, NT02, and NT03 of 0.55%, 2.3%, and 3.4%, respectively. Thus, it is possible to use the Petukhov correlation, which was developed for pure fluids in single-phase flow, to predict the pressure drop in low-concentration nanofluids using the appropriate thermophysical properties of the desired nanofluid.

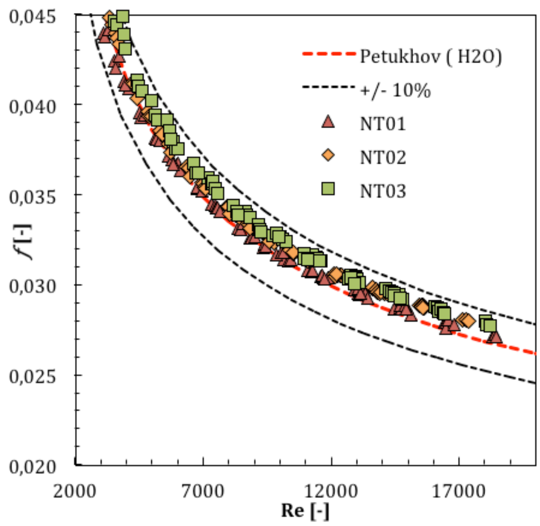

Figure 11: Experimental results of the Darcy's friction factor, f_{exp} versus Reynolds number, for three nanofluids (NT01, NT02 and NT03), including the Petukhov correlation for distilled water.

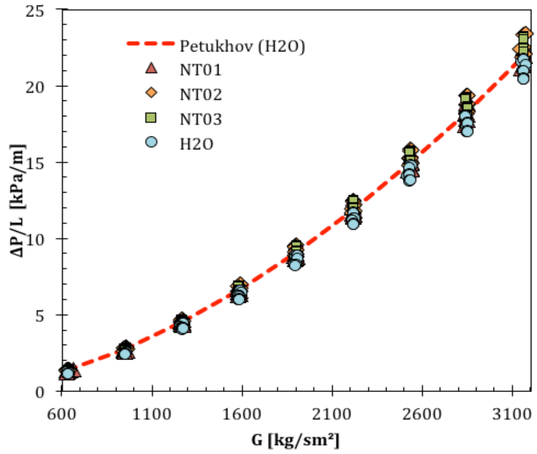

Figure 12: Test section pressure gradient versus mass velocity for all samples.

The experimental results for the pressure drop of the fluid flow between the inlet and outlet of the test section are shown in Fig. 12 as a function of the mass velocity, G. All the nanofluid samples showed pressure drop values greater than that of the base fluid. Sample NT01 showed a pressure drop that was, on average, 5.6% greater than that of the base fluid, which emphasizes that the viscosity of this sample resulted in an increase of 8.6% compared with distilled water. However, the increase in the pressure drop for samples NT02 and NT03 with a higher volume concentration (0.24%) was, on average, 8.7% and 8.6%, respectively, greater than that of the base fluid, which emphasizes that the increase in the viscosity for these two samples was, on average, 17.8% and 11.6%, respectively, relative to that of distilled water.

3.3 Thermal-hydraulic Performance

The thermal-hydraulic performance of the three nanofluid samples was evaluated, determining the increase in the convective heat transfer coefficient as a function of the pumping power consumed in the test section, as illustrated in Eq. (11) for the same test conditions.

$$\dot{W}_p = \frac{\dot{m}_{nf}\Delta P}{\rho_{nf}} \tag{11}$$

Figure 13 shows a comparison of the results shown in the present study with those obtained by (Haghighi *et al.*,2014), for nanofluids made from Al2O3/water and TiO2/water and the results from (Meyer *et al.*, 2013), for nanofluids made from MWCNT/water for the turbulent flow region.

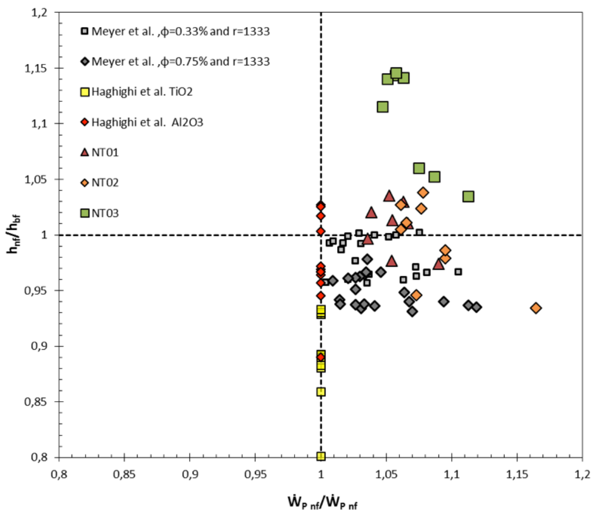

Figure 13: Comparison of the thermal hydraulic performance for all samples tested, including the experimental results from Haghighi et al. (2014) and Meyer et al. (2013).

(Meyer *et al.*, 2013), concluded that the tested nanofluid is not ideal for applications such as a cooling fluid in turbulent flow, which is verified in Fig. 13, where their experimental points are found in the fourth quadrant, thus confirming an unsatisfactory thermal-hydraulic performance. According to the authors, adopting the evaluation criteria of (Prasher *et* *al*., 2006), who considered a conservative case when the Nusselt number of the nanofluid is equal to that of the base fluid, the increase in the viscosity cannot be greater than four times the increase in the thermal conductivity. In the case of the results presented by (Meyer *et al*., 2013) , this relationship was approximately 8.5 times. For the samples tested in the present study, all showed values of less than 4, particularly sample NT03, where the relationship was 1.3 times. Finally, the NT03 sample, with an aspect ratio of r=2400 and a concentration of 0.24%, showed promising thermal-hydraulic performance since it had increases in the convective heat transfer coefficient that were greater than 15% and, in relation to the pumping power, increases that were less than 10%.

4. CONCLUSIONS

The experimental results obtained in the present work permitted the following conclusions:

- In general, the thermal conductivity of the nanofluids, primarily those with a higher volumetric concentration (0.24%), was greater than that of the base fluid. The NT03, with the largest aspect ratio, 2400, presented the largest increase in the thermal conductivity, 17%, relative to the base fluid.
- The results showed that the viscosity obtained for the nanofluids was greater than that for distilled water, with the largest increase in viscosity of 17.8% obtained for NT02.
- The NT03 showed the largest increase in the heat transfer coefficient (~6%) when compared as a function of mass velocity and an increase of 30% as a function of the Reynolds number.
- Regarding the pressure drop, the sample with the lowest concentration, NT01, exhibited an increase of 5.6% relative to the base fluid, whereas samples NT02 and NT03 exhibited increases of 8.7% and 8.6%, respectively, relative to that of distilled water.
- The thermal-hydraulic performance was also evaluated, which related the heat transfer coefficient and the pumping power. The NT03 showed promising performance, with an increase in the heat transfer coefficient greater than 15% and an increase in pumping power of less than 10%, related to the base fluid.

5. ACKNOWLEDGMENT

The authors gratefully acknowledge the support given to this investigation by CAPES, CNPq and Fapemig.

6. REFERENCES

Asirvatham L.G., Raja B., Mohan Lal D., Wongwises S., 2011. Convective heat transfer of nanofluids with correlations, Particuology 9, (6) ,626-631.

Bandarra Filho E.P., Mendoza O.S.H., Beicker C.L.L., Menezes A., Wen D., (2014). Experimental investigation of a silver nanoparticle-based direct absorption solar thermal system, Energy Conversion and Management 84 ,261-267.

Choi S.U.S.,1995. Enhancing thermal conductivity of fluids with nanoparticles, in Proceedings of the 1995 ASME International Mechanical Engineering Congress and Exposition, (ASME, 1995), vol. 231, pp. 99-105.

Gnielinski V., 1976. "New equations for heat and mass transfer in turbulent pipe and channel flow", Forschung im Ingenieurwesen 16, 359-368.

Haghighi E.B. et al., (2014). Experimental Study on Convective Heat Transfer of Nanofluids in Turbulent Flow: Methods of Comparison of Their Performance, Experimental Thermal and Fluid Science 57 , 378-387.

Masuda H., Ebata A., Teramae K., Hishinuma N. ,1993. Alteration of thermal conductivity and viscosity of liquid by dispersing ultra-fine particles. Dispersion of Al_2O_3, SiO_2 and TiO_2 ultra-fine particles, Netsu Bussei 7 227-233.

Meyer J.P., McKrell T.J., Grote K., 2013. The influence of multi-walled carbon nanotubes on single-phase heat transfer and pressure drop characteristics in the transitional flow regime of smooth tubes, Int .J. Heat Mass. 58, 597-609.

O'Hanley H., Buongiorno J., McKrell T., Hu L.-wen, 2012. Measurement and model validation of nanofluid specific heat capacity with differential scanning calorimetry, Advances in Mechanical Engineering 2012 , 1-6.

Pak B.C and Cho Y.I, 1998 . Hydrodynamic and heat transfer study of dispersed fluids with submicron metallic oxide particles, Experimental Heat Transfer 11,151-170.

Petukhov B.S and Popov V.N., 1963. Theoretical calculation of heat exchange and frictional resistance in turbulent flow in tubes of an incompressible fluid with variable physical properties, High Temp. 1 , 69–83.

Prasher R., Song D., 2006. Wang J., Phelan P., Measurements of nanofluid viscosity and its implications for thermal applications, Applied Physics Letters 89 (13).

Sajadi A.R and Kazemi M. H., 2011. Investigation of turbulent convective heat transfer and pressure drop of TiO_2/water nanofluid in circular tube, International Communications in Heat and Mass Transfer, 38 (10) ,1474-1478

Sundar L.S., Naik M.T., Sharma K.V., Singh M.K., Siva T.C., (2012). Experimental investigation of forced convection heat transfer and friction factor in a tube with Fe_3O_4 magnetic nanofluid, Exp. Thermal and Fluid Sci. 37 ,65-71.

Xuan Y. and Li Q., 2003. Investigation on Convective Heat Transfer and Flow Features of Nanofluids. Journal of Heat Transfer, 125 (1) ,125-151.